Combining Two-level Data Structures and Line Space Precomputations to Accelerate Indirect Illumination

K. Keul, T. Koß, F. L. Schröder and S. Müller
Institute for Computational Visualistics, University of Koblenz-Landau, Germany

Keywords: Visualization, Ray Tracing, Data Structures.

Abstract: We present a method for combining two-level data structures and directional precomputation based on the Line Space (LS). While previous work has shown that LS precomputation significantly improves ray traversal performance of typical spatial data structures, it suffers from high memory consumption and low image quality due to internal approximations. Our method combines this technique with two-level BVHs, where the LS is integrated within second-level object BVHs. The advantages are, among others, optimizations in terms of approximation accuracy and required memory. In addition, we propose a method to use an accurate BVH in combination with the fast approximation-based LS for path tracing in order to further reduce image errors of the LS while still benefitting from its gain in performance.

1 INTRODUCTION

Besides ray tracing acceleration through spatial data structures, there have been many attempts based on directional visibility information. Recently, the Line Space (LS) was proposed as extension of spatial structures (Keul et al., 2016) (Billen and Dutré, 2016). There, rays are clustered and classified within shafts during initialization. A representative candidate was used per shaft, which acted as blocker approximation during runtime (Keul et al., 2018). This accelerated ray traversal significantly, however, at the cost of approximation-based errors in the resulting image and high memory consumption.

In the context of object instancing and rigid object movements, two-level structures are employed, which build a top-level structure around second-level object structures. Their performance is in general inferior compared to their single-level flat counterparts (Benthin et al., 2017). With this work, we first propose a combination of two-level BVHs and representative candidate LS precomputations to combine the advantages of both. Typically, second-level object bounding volumes of two-level structures are small and tightly-fit to the contained objects. This property makes LS approximations more accurate and reduces image errors, as demonstrated in figure 1. In addition, less LS nodes need to be generated and therefore less memory is consumed, especially in scenes that rely on object instancing.

In a second step, we propose a method for combining different data structures in path tracing systems. While BVHs are used on earlier path segments, where accurate results are needed, approximation-based LS

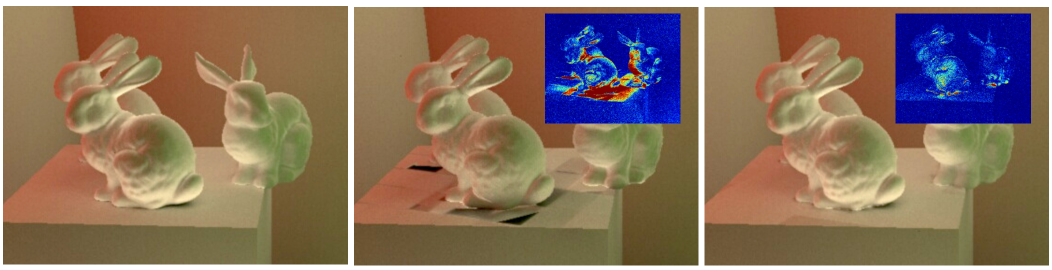

Figure 1: Improvements in indirect lighting calculation. We combine two-level BVHs with an approximation-based representative candidate Line Space (2L-LS). Even with a lower depth parameter (in brackets), we achieve less approximation errors compared to a LS integrated in a single-level flat BVH (F-LS). Additionally, less errors appear when used in later bounces.

Keul, K., Koß, T., Schröder, F. and Müller, S.
Combining Two-level Data Structures and Line Space Precomputations to Accelerate Indirect Illumination.
DOI: 10.5220/0007345902280235
In *Proceedings of the 14th International Joint Conference on Computer Vision, Imaging and Computer Graphics Theory and Applications (VISIGRAPP 2019)*, pages 228-235
ISBN: 978-989-758-354-4

results are used in later path segments, where accuracy is less relevant. By this, errors in the final image are nearly eliminated and the fast performance of the LS can be used almost without any drawbacks in image quality.

2 RELATED WORK

Indirect lighting calculation and ray tracing systems are extensively studied topics, which are well presented in previous work (Ritschel et al., 2012)(Pharr et al., 2016). Acceleration structures for ray tracing have been researched intensively as well. Hence, we present a brief overview of the most relevant literature in the most related topics of our work. We focus on bounding volume hierarchies (BVHs), as current research suggests, that these result in the highest ray tracing performance (Havran, 2000) (Zlatuška and Havran, 2010) (Vinkler et al., 2016).

Bounding Volume Hierarchies. Since the first automatic construction algorithm of BVHs was published (Kay and Kajiya, 1986), many extensions and optimizations for BVHs have been proposed (Aila et al., 2012) (Aila et al., 2013). Most construction algorithms work in a top-down manner, splitting the scene along a promising plane in order to narrow the domain of scene triangles that need to be tested for intersection during runtime (Wald, 2007) (Wald, 2012). Spatial splits in the BVH (called SBVH) are used for better arrangement of the bounding volumes, but lead to higher depths in the hierarchy (Stich et al., 2009). More recently, SBVHs were optimized for better SIMD parallelization (Fuetterling et al., 2016), improved subdivision of the scene triangles (Ganestam and Doggett, 2016) and better split cost prediction through temporarily constructed BVHs (Wodniok and Goesele, 2017). These approaches result in high quality BVH trees with good performance but higher and mostly non-interactive construction time.

Construction algorithms based on Morton codes result in interactive build times with the hierarchical linear BVH (HLBVH) (Lauterbach et al., 2009) (Pantaleoni and Luebke, 2010) (Garanzha et al., 2011). Recent advances extend Morton codes by also encoding the object size and using adaptive axis order and bit size to improve the handling of non-uniform scene distribution (Vinkler et al., 2017). Morton codes were also used to cluster scene primitives with a parallel approximate agglomerative clustering method (Gu et al., 2013) (Meister and Bittner, 2017). Further, the Bonsai algorithm was proposed, where subtrees are later gathered by a top-tree (Ganestam et al., 2015). Recent methods start from fast-initialized HLBVHs that are optimized afterwards. This can be done by consequent remove-and-insert updates (Bittner et al., 2013) (Meister and Bittner, 2018), optimization of the spatial splits (Hendrich et al., 2017) or subsequent parallel treelet optimization (Karras and Aila, 2013).

Two-level Data Structures. It is also possible to use a two-level subdivision scheme with second-level object hierarchies and a top-level structure that is built on top of these objects. While the tree quality is typically worse in comparison to flat (i.e. single-level) structures, which is due to the irregular tree depth, two-level approaches grant some benefits. Therein, dynamic scenes with rigid object animation are implemented through transformation of the previously built object hierarchies. Object instancing results in less memory consumption, as the data structure used per object can be reused. This technique was first proposed for k-d-trees (Wald et al., 2003), but since also applied to other data structures like grids (Kalojanov et al., 2011) and BVHs in OptiX (Parker et al., 2010) and Embree (Wald et al., 2014). However, overlapping object hierarchies lead to multiple objects that need to be tested for intersections in order to find the nearest intersection point. For this disadvantage, two-level BVHs were extended by using partial re-braiding (Benthin et al., 2017), which opens and merges overlapping object BVHs during runtime. Also, in comparison to its flat counterpart, the tree structure of two-level structures is less balanced, which results in inferior SIMT parallelization when traversing different objects. This disadvantage is regarded in our approach, as the Line Space is able to limit the maximum depth of object BVHs to a fixed level, leading to more balanced hierarchies.

Visibility Structures. In terms of directional data structures, the accumulation of rays to beams is known as beam tracing and was shown to result in good performance, however, at the cost of high memory consumption and initialization time (Reshetov et al., 2005) (Mortensen et al., 2007) (Laine et al., 2009). The general approach is to generate multidimensional visibility fields around scene objects, granting precomputed classification schemes for the contained rays. These methods are for instance used in radiosity systems (Cohen and Wallace, 2012) or for accelerated computation of indirect illumination in ray tracing (Gaitatzes et al., 2010), sometimes based on approximated results (Bashford-Rogers et al., 2011).

Newer work introduces the Line Space (LS) as a classification scheme for rays, which groups the rays into shafts within a regularly subdivided bounding box, based on top of a spatial data structure (Keul et al., 2016) (Billen and Dutré, 2016). Information is precomputed based on shafts and applied to all contained rays during runtime. This was used as an acceleration structure on top of grids and BVHs for approximate soft shadow and indirect lighting calculations (Keul et al., 2017) (Keul et al., 2018). While the resulting images have visible artifacts due to the shaft approximations, it was shown that some artifacts are negligible when approximations are only used for indirect lighting computations (Yu et al., 2009). With this, the LS is one magnitude faster in ray tracing performance in comparison to typical data structures. Besides the image quality, the main disadvantages are the extensive memory usage and build time that arise from the high number of precomputed shafts.

3 TWO-LEVEL LINE SPACE

An observation, used in our work, is that approximation accuracy is higher, when smaller and more tightly-fitting bounding volumes are used for the LS. For this purpose, we adapt the LS to two-level BVHs that grant smaller bounding volume sizes in second-level object BVHs, leading to higher LS precision. We first revise the representative candidate LS technique as proposed by (Keul et al., 2018). Afterwards, we describe the adaption to two-level BVHs, which is one of the main contributions of this paper. Lastly, we give a short discussion of all parameters involved.

3.1 Representative Candidate LS

Tracing cost is dividable in traversal cost of the underlying tree and cost of intersection tests that are made to find the intersected scene primitive. The representative candidate LS finds characteristic intersection candidates for shafts during initialization. With this, the tree traversal is cut at a specific level, where the representative candidate LS nodes are integrated. Then, instead of calculating intersection tests between rays and geometric scene primitives, the precomputed representative shaft candidate approximates the ray intersection within that shaft. While this improves performance remarkably, the candidate approximation leads to visible errors.

The initialization of the representative candidate LS is straightforward. First, the underlying spatial data structure (i.e. the BVH) is constructed. Then a LS node is constructed for every node in a given depth of the underlying BVH. A LS node is a bounding volume, where all sides of the bounding box surface are subdivided into equally sized patches. Every two distinctive patches are joined to result in a shaft connecting those patches. Hence, each ray through

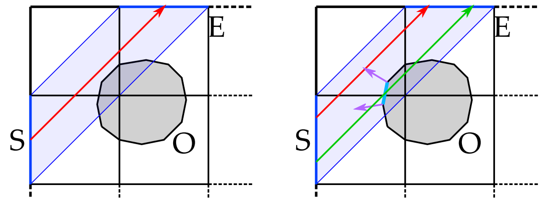

Figure 2: Initialization with representative shaft candidate search. If the midpoint ray of the shaft between patches S and E has no intersection (left), further rays are used (right).

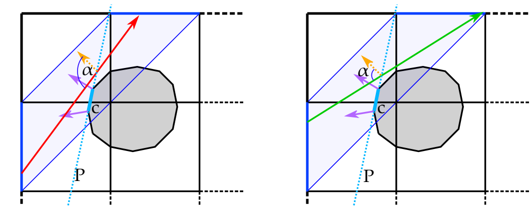

Figure 3: Runtime usage of the shaft candidate c. It is used as "infinite plane" P for all rays of the shaft. If angle α between a ray and the extrapolated normal (yellow) is too big, blocker approximation is refused (left). Otherwise it is used, even with no actual object intersection (right).

the bounding volume can be assigned to a single shaft. In the representative candidate LS every shaft has a triangle reference, which describes the surface of the scene primitives covered by the shaft. The triangle (the representative candidate) is found by simple ray traversal within the underlying data structure during initialization. The ray used for traversal is determined by the midpoints of the patches that represent the shaft. If this ray has no intersection, additional rays can be traced. If still no intersection was found, the shaft is declared as empty. This process is shown in figure 2. During runtime, the representative candidate is used as a blocker approximation for all rays of the given shaft, resulting in an "infinite plane". However, if the extrapolated normal of the approximation exceeds a given threshold, a potential boundary of the contained object can be assumed, as illustrated in figure 3. The approximation is then discarded and traversal continues.

3.2 Two-level LS Structure

The main idea of our work is to combine the LS with previously generated two-level BVHs, that arrange logical scene objects on the first level and involve scene primitives only within the second level. The second-level object BVH nodes have a tighter fit to their content, which makes them smaller in size and more beneficial for the LS. This reduces the total number of LS nodes needed while simultaneously improving approximation accuracy. We differentiate four different setups of the data structure, as also vi-

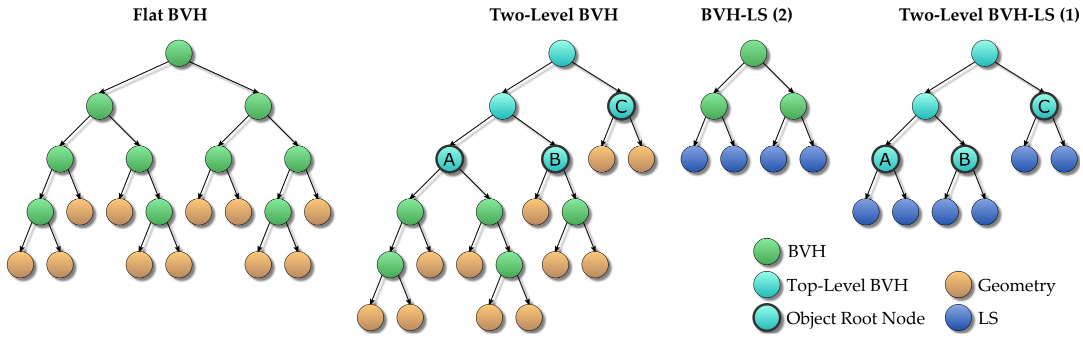

Figure 4: Acceleration structures used. Flat BVHs are the most common structures. Two-level BVHs are used for rigid object dynamics, granting minimal tree updates for object movements but worse runtime performance. The LS improves performance, due to early approximation-based traversal termination. Our work combines the LS and two-level BVHs, to gain fast performance and higher approximation accuracy. The numbers show the integration depth within (object-) hierarchies.

sualized in figure 4:

1. Flat BVH, as state-of-the-art ray tracing structure;
2. Two-level BVH, better suited for rigid object dynamics and instancing, but with higher tree complexity and lower runtime performance;
3. Flat BVH with LS integration, for fast blocker approximations, but with higher memory consumption and visible errors due to approximation, as in (Keul et al., 2018);
4. Two-level BVH with LS integration, same advantages as two-level BVHs and flat BVH-LS, with less approximation errors, presented in our work.

The LS adaption improves second-level object BVHs with LS nodes, that are integrated in a specific hierarchy depth. Similar to other two-level structures, the two-level LS is well suited for rigid object dynamics and instancing. This way, every unique logical object contains its own BVH-LS, whereas the top-level hierarchy stores references to those object structures in its leafs. Therefore, the two-level LS benefits significantly from object instancing, as every memory consuming LS is only stored once per geometrical object. Our results further demonstrate, that the performance benefit gained through LS approximations outperforms traditional BVHs, even when used in typically slower two-level data structures. Because of the tighter fit to contained objects, the two-level LS improves approximation accuracy, even when less nodes are generated and less memory is consumed. These theoretical considerations are summarized in table 1.

As shown in figure 4, two-level structures in general result in more unbalanced and partly deeper tree hierarchies compared to their flat counterpart. This is especially problematic when complex and simple objects are used simultaneously. During SIMT traversal, kernels are not able to benefit from thread coherency, which decelerates the overall traversal step.

Table 1: Expected results for the data structures. In terms of quality, flat BVHs and two-level BVHs give correct results, while LS techniques have better runtime performance.

	Memory	Performance	Quality
F-BVH	★★★	★★☆☆	★★★
2L-BVH	★★★	★☆☆☆	★★★
F-LS	★☆☆	★★★★	★☆☆
2L-LS	★★☆	★★★☆	★★☆

Our technique represents a solution to this two-level imbalance, as the LS limits the maximum object hierarchy depth to a specified level. This, along with the approximation-based early ray termination, improves SIMT thread coherency and traversal performance, due to less overhead caused by bad thread parallelism. Concerning BVH initialization, any of the existing construction or optimization algorithms can be used. However, bad BVH quality in general results in larger bounding volumes, leading to bigger shafts and therefore worse LS approximation accuracy. Consequently, a high-quality BVH builder generates a lower number of nodes, that additionally have better scene coverage and are smaller in size, which improves runtime performance and approximation accuracy. Hence, less LS nodes are needed for better quality and runtime performance. As the top-level BVH has no connection to the LS, it can be created with any build algorithm.

3.3 Parameter Discussion

As in previous work, there are two different parameters for our technique: the LS integration depth and the subdivision parameter. The integration depth is the depth within the base structure that stores LS nodes instead of children information. A higher depth results in a deeper hierarchy, more LS nodes and therefore higher memory consumption and lower run-

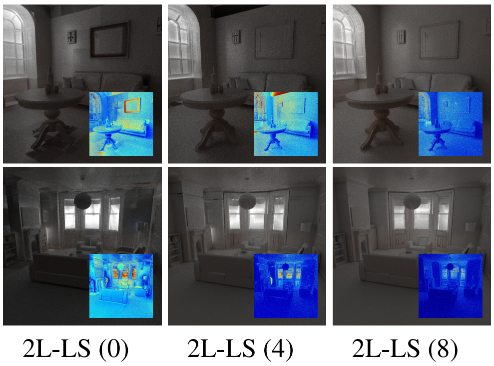

Figure 5: Indirect lighting results of different LS integration depths (marked in brackets - 0 means root node stores LS). Higher depths grant better approximations and less errors. As shown, the needed integration depth is scene dependent.

time performance. However, image quality improves, due to higher shaft precision. This is demonstrated in figure 5. The subdivision parameter N determines LS accuracy. Shafts are created from the surface patches of the node's subdivided bounding volume. Higher subdivision leads to smaller patches and therefore thinner shafts and more precise approximations. Nevertheless, significantly more shafts are generated and more memory is consumed. In agreement with previous work, we favor two different parameter values for N, targeting either low memory consumption ($N = 6$) or higher approximation accuracy ($N = 10$). The differences in quality are presented in figure 8.

4 PATH TRACING WITH MULTIPLE DATA STRUCTURES

The early traversal termination with candidate approximation of the LS leads to a significant improvement in tracing performance, however, at the cost of approximation errors. By using an adequate parameter set, these errors can be greatly reduced, while in turn memory consumption increases tremendously. Keeping this in mind, our goal is to use different parameter sets and data structures in different segments of path tracing. With this, we can use the BVH, in situations that need correct results and the LS with different parameter sets depending on whether the focus lies on accuracy or tracing performance.

During path tracing, there are several ways to determine, whether a ray can be approximated or should be calculated accurately. It is possible to use the evaluation of the probability density function of the current path segment or to distinguish its type, i.e. whether a shadow, reflected or diffuse ray is evaluated. For simplicity, we make this distinction based on the bounce depth of the current path segment in a backward path tracing system. There, the first bounce (indirect illumination through one object) and its according shadow ray are calculated correctly with a BVH. The second bounce (indirect illumination with two intermediate objects) is less relevant and therefore calculated with the faster approximation-based LS. Further rays have decreasing relevance in illumination and are calculated with a lower-quality higher-performance LS. This process is illustrated in figure 6 and with the resulting errors demonstrated in figure 7. Primary rays and the according shadow rays can be rendered with rasterization-based approaches, which are fast and generate correct results.

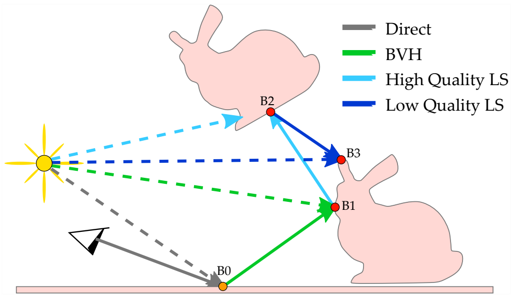

Figure 6: 3-bounce path using different data structures depending on the bounce depth. Primary and direct shadow rays use rasterization techniques. BVH path segments have precise results, while LS segments are traced faster.

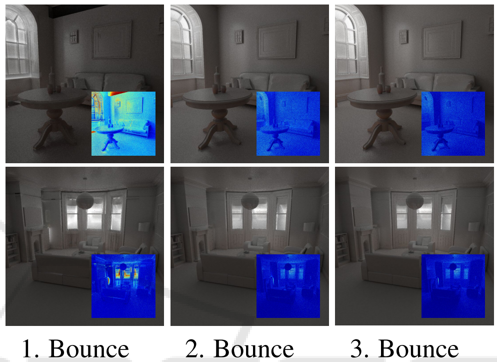

Figure 7: Results of different bounce depths of LS usage. The number marks the path depth, from which on approximation-based LS (2L-LS (4)) is used. Later usage of LS results in less errors as well as less performance gain.

5 RESULTS

We tested and compared our two-level LS approach (2L-LS) as approximation-based method for indirect lighting calculation. Our test setup is comparable to (Keul et al., 2018), where the single-level flat BVH-

Table 2: Construction results of the single-level flat BVH-LS (F-LS) and the two-level BVH-LS (2L-LS) in terms of the total number of generated LS, memory consumption (in MB) and build time (in s). The integration depths are shown in brackets.

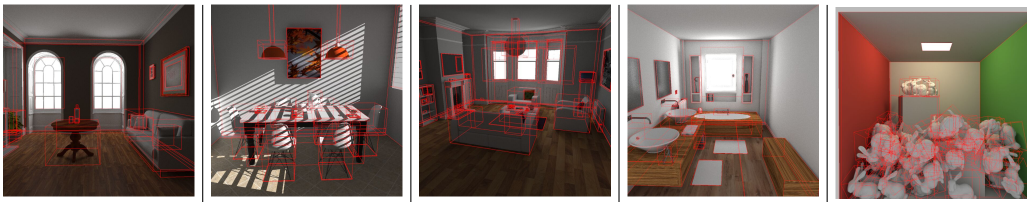

	FIREPLACE 143k triangles 49 objects			BREAKFAST 269k triangles 45 objects			LIVING ROOM 576k triangles 78 objects			SALLE DE BAIN 1231k triangles 39 objects			BUNNY SCENE 4467k triangles 64 instances		
Structure	**#LS**	**MB**	**s**	**#LS**	**MB**	**s**	**#LS**	**MB**	**s**	**#LS**	**MB**	**s**	**#LS**	**MB**	**s**
$N = 6, \approx 38k$ shafts per LS															
F-LS (8)	226	28.1	0.82	186	26.4	1.58	198	38.4	1.58	207	53.4	3.07	245	141.2	10.29
F-LS (10)	763	80.9	2.17	641	70.8	4.11	620	81.5	2.77	706	98.0	4.97	954	199.5	13.05
F-LS (12)	2223	206.0	5.83	2185	214.3	12.49	1936	199.1	6.33	2628	238.7	11.90	3750	407.4	23.78
2L-LS (0)	49	8.4	0.81	45	11.0	1.11	78	22.8	1.95	39	35.5	2.64	9	2.5	0.24
2L-LS (4)	526	53.4	1.62	648	68.5	2.89	940	109.2	3.60	467	76.1	3.87	24	3.8	0.29
2L-LS (8)	4195	344.9	8.27	7351	646.5	21.78	7373	631.7	15.92	6296	490.5	18.55	264	20.2	0.98
$N = 10, \approx 300k$ shafts per LS															
F-LS (4)	16	18.0	0.52	16	21.8	1.12	16	29.6	1.36	16	46.9	2.59	16	132.9	9.83
F-LS (6)	63	57.2	1.24	54	51.4	2.70	59	70.1	2.05	59	85.1	3.31	63	170.9	11.01
F-LS (8)	226	184.8	3.78	186	147.1	7.89	198	190.6	4.31	207	194.2	6.66	245	294.4	15.39
2L-LS (0)	49	38.0	1.24	45	35.8	2.05	78	74.7	2.71	39	62.3	3.21	9	7.0	0.30
2L-LS (4)	526	366.7	6.50	648	450.0	14.10	940	708.4	12.66	467	362.1	10.45	24	16.7	0.59
2L-LS (6)	1634	1058.4	19.62	2328	1549.6	47.93	2931	1926.1	37.25	1719	1079.0	32.82	72	42.6	1.49

LS (F-LS) was proposed, which is our main competitor in terms of performance. For a complete evaluation we also compare against the pure underlying structures (F-BVH and 2L-BVH) which produce approximation-free results. For all BVH algorithms we use state-of-the-art techniques targeting good tree quality and fast runtime performance, as shown in (Aila et al., 2012). We compare all methods in terms of traversal performance, memory consumption and build time. Additionally, we compare the approximation-based results per bounce to ground truth data and show, that approximations produced by our technique are more precise than those of F-LS.

The chosen test scenes are commonly used architectural scenes (FIREPLACE ROOM, BREAKFAST ROOM, LIVING ROOM and SALLE DE BAIN) and a scene with instanced objects (BUNNY SCENE). These scenes consist of multiple manually separated objects, which are used as second-level object BVHs, as shown in table 3. We use a multiple-bounce path tracing system for indirect lighting calculation with different data structures that can be used in different path depths, as explained in section 4. Image resolution was 1024×1024. Primary and direct shadow rays are not computed via ray tracing, as there are faster rasterization-based approaches. The test system consists of an Intel i7-6800k 3.6 GHz CPU and a NVidia GeForce GTX 1080 GPU using GLSL Compute Shaders. To guarantee a fair comparison of the used data structures, we do not use any third party implementations. Overall, the presented results confirm the theoretical considerations from section 3.2.

Table 3: Path tracing performance and per bounce error of varying LS integration depth (in brackets) and subdivision parameter (N) averaged over all scenes.

ALL SCENES	**Perf**	**RMSE on Bounce**		
Structure	**MRays/s**	**1**	**2**	**3**
F-BVH	70.7	–	–	–
2L-BVH	34.3	–	–	–
F-LS (8), $N = 6$	377.0	.030	.011	.004
F-LS (10), $N = 6$	313.0	.025	.008	.002
F-LS (12), $N = 6$	268.3	.021	.006	.002
2L-LS (0), $N = 6$	208.0	.023	.008	.003
2L-LS (4), $N = 6$	120.2	.012	.004	.002
2L-LS (8), $N = 6$	92.5	.009	.003	.002
F-LS (4), $N = 10$	622.6	.044	.019	.006
F-LS (6), $N = 10$	440.6	.033	.012	.004
F-LS (8), $N = 10$	346.6	.018	.007	.002
2L-LS (0), $N = 10$	201.8	.015	.005	.002
2L-LS (4), $N = 10$	117.7	.008	.003	.001
2L-LS (6), $N = 10$	102.2	.006	.002	.001

Table 2 shows construction results of our method compared to the single-level LS. We used two different subdivision parameters ($N = 6$ and $N = 10$) and three different integration depths, leading to mostly similar memory consumption for all data structures, which makes them comparable. Obviously, memory usage and build time are dependent on the total number of nodes containing LS information. Hence, scenes using object instancing have significantly less memory consumption and by far lower build times in two-level structures, as shown by the BUNNY SCENE.

Table 3 and figures 1 and 8 show the runtime

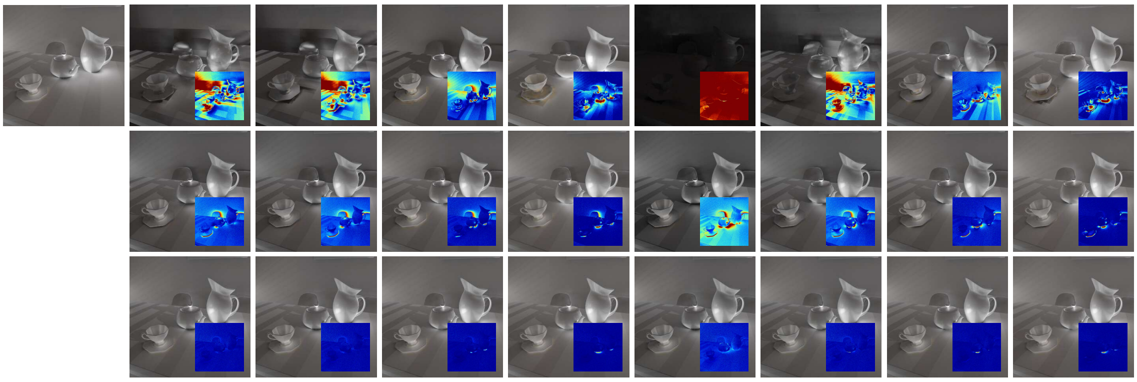

Figure 8: Per bounce results of F-LS and 2L-LS using different parameter sets. Obviously, higher integration depths (in brackets) and subdivision parameters (N) lead to less errors in the resulting images. In turn, higher parameters in general result in larger memory consumption, as illustrated by table 2. The exact performance and error values are shown in table 3.

results, i.e. tracing performance and error values for indirect rays. Approximation-based errors produced by the LS are specified by RMSE (root-mean-squared error) values, based on the per-pixel differences to ground truth data. The bounce depth marks the depth from which on the shown data structure is used - earlier bounces use the BVH for correct results. It is noticeable, that later bounces traced with approximation-based LS structures lead to insignificant errors but much faster tracing performance. Two-level structures in general have inferior performance in comparison to their single-level flat counterparts, as explained in section 3.2. In turn, they produce less errors in general, even with lower depth integration parameters. Our results also show that higher subdivision parameters need significantly more memory and therefore lower integration depths are used, which in turn reduces approximation accuracy leading to worse image results. Due to this, higher subdivision parameters are more suitable for later path segments, in which the lower integration depth leads to better performance, while the higher subdivision preserves accuracy to a higher degree. Summarized results for different data structures used in different bounces, averaged over all scenes, are shown in table 4.

Table 4: Summarized path tracing results with different data structures for different path segments averaged over all scenes. Used LS structures are: 2L-LS 1 = 2L-LS(4) $N = 6$, 2L-LS 2 = 2L-LS(0) $N = 10$, F-LS = F-LS(8) $N = 6$.

Data Structure in bounce			**Average of all scenes (tables 2 and 3)**		
1	**2**	**3**	**Memory (MB)**	**MRays/s**	**RMSE**
F-BVH	F-BVH	F-BVH	21.0	70.7	–
F-BVH	F-BVH	2L-LS 1	83.2	87.2	.002
F-BVH	2L-LS 1	2L-LS 1	83.2	103.7	.004
F-BVH	2L-LS 1	2L-LS 2	126.8	130.9	.004
F-BVH	2L-LS 2	2L-LS 2	64.6	158.1	.005
F-BVH	2L-LS 1	F-LS	140.7	189.3	.006
F-BVH	F-LS	F-LS	78.5	274.9	.011

6 CONCLUSION

We proposed a novel combination of two-level BVHs and recently introduced LS approximations. We explained how the combination benefits from both of their advantages, while also reducing their disadvantages. The object-level LS reduces approximation errors and increases tracing performance by limiting the integration depth. Consequently, our approach results in better runtime performance compared to traditional BVHs, with less memory consumption and approximation errors compared to single-level LS structures. Furthermore, we presented a method to connect the strengths of different structures in a multiple-bounce path tracing system, with a per bounce selection that indicates, whether accurate BVH or fast approximation-based LS results are used.

In an extensive evaluation we presented the usefulness of these approaches, showing different parameters and per bounce results for the flat BVH-LS and two-level BVH-LS combination and compared the results with state-of-the-art techniques. In that, our evaluation shows that our two-level approach is an improvement of the flat technique. Moreover, the two-level approach makes LS approximations usable in scenes with rigid object animations and especially useful coupled with object instancing. Finally, the per bounce usage reduces approximation errors at a high level, while at the same time enables better LS usage in combination with traditional data structures.

REFERENCES

Aila, T., Karras, T., and Laine, S. (2013). On quality metrics of bounding volume hierarchies. In *Proc. High Performance Graphics*.

Aila, T., Laine, S., and Karras, T. (2012). Understanding the efficiency of ray traversal on gpus–kepler and fermi addendum. *NVIDIA Technical Report*.

Bashford-Rogers, T., Debattista, K., Harvey, C., and Chalmers, A. (2011). Approximate visibility grids for interactive indirect illumination. In *Conf. Games and Virtual Worlds for Serious Applications*.

Benthin, C., Woop, S., Wald, I., and Áfra, A. T. (2017). Improved two-level bvhs using partial re-braiding. In *High Performance Graphics*.

Billen, N. and Dutré (2016). Visibility acceleration using efficient ray classification. *Department of Computer Science, KU Leuven*.

Bittner, J., Hapala, M., and Havran, V. (2013). Fast insertion-based optimization of bounding volume hierarchies. In *Computer Graphics Forum*.

Cohen, M. F. and Wallace, J. R. (2012). *Radiosity and realistic image synthesis*. Elsevier.

Fuetterling, V., Lojewski, C., Pfreundt, F.-J., and Ebert, A. (2016). Parallel spatial splits in bounding volume hierarchies. In *Eurographics Symposium on Parallel Graphics and Visualization*.

Gaitatzes, A., Andreadis, A., Papaioannou, G., and Chrysanthou, Y. (2010). Fast approximate visibility on the gpu using precomputed 4d visibility fields. *WSCG*.

Ganestam, P., Barringer, R., Doggett, M., and Akenine-Möller, T. (2015). Bonsai: rapid bounding volume hierarchy generation using mini trees. *Computer Graphics Techniques 4*.

Ganestam, P. and Doggett, M. (2016). Sah guided spatial split partitioning for fast bvh construction. In *Computer Graphics Forum*.

Garanzha, K., Pantaleoni, J., and McAllister, D. (2011). Simpler and faster hlbvh with work queues. In *Proc. High Performance Graphics*.

Gu, Y., He, Y., Fatahalian, K., and Blelloch, G. (2013). Efficient bvh construction via approximate agglomerative clustering. In *Proc. High Performance Graphics*.

Havran, V. (2000). *Heuristic ray shooting algorithms*. PhD thesis, Czech Technical University in Prague.

Hendrich, J., Meister, D., and Bittner, J. (2017). Parallel bvh construction using progressive hierarchical refinement. In *Computer Graphics Forum*.

Kalojanov, J., Billeter, M., and Slusallek, P. (2011). Two-level grids for ray tracing on gpus. In *Computer Graphics Forum*.

Karras, T. and Aila, T. (2013). Fast parallel construction of high-quality bounding volume hierarchies. In *Proc. High Performance Graphics*.

Kay, T. L. and Kajiya, J. T. (1986). Ray tracing complex scenes. *SIGGRAPH Comput. Graph.*

Keul, K., Klee, N., and Müller, S. (2017). Soft shadow computation using precomputed line space visibility information. *Journal of WSCG*.

Keul, K., Koß, T., and Müller, S. (2018). Fast indirect lighting approximations using the representative candidate line space. *Journal of WSCG*.

Keul, K., Müller, S., and Lemke, P. (2016). Accelerating spatial data structures in ray tracing through precomputed line space visibility. *WSCG*.

Laine, S., Siltanen, S., Lokki, T., and Savioja, L. (2009). Accelerated beam tracing algorithm. *Applied Acoustics*.

Lauterbach, C., Garland, M., Sengupta, S., Luebke, D., and Manocha, D. (2009). Fast bvh construction on gpus. In *Computer Graphics Forum*.

Meister, D. and Bittner, J. (2017). Parallel locally-ordered clustering for bounding volume hierarchy construction. *IEEE Trans. on Visualization and Computer Graphics*.

Meister, D. and Bittner, J. (2018). Parallel reinsertion for bounding volume hierarchy optimization. In *Computer Graphics Forum*.

Mortensen, J., Khanna, P., Yu, I., and Slater, M. (2007). A visibility field for ray tracing. In *Computer Graphics, Imaging and Visualisation*.

Pantaleoni, J. and Luebke, D. (2010). Hlbvh: hierarchical lbvh construction for real-time ray tracing of dynamic geometry. In *Proc. High Performance Graphics*.

Parker, S. G., Bigler, J., Dietrich, A., Friedrich, H., Hoberock, J., Luebke, D., McAllister, D., McGuire, M., Morley, K., Robison, A., et al. (2010). Optix: a general purpose ray tracing engine. *ACM Transactions on Graphics (TOG)*.

Pharr, M., Jakob, W., and Humphreys, G. (2016). *Physically based rendering: From theory to implementation*. Morgan Kaufmann.

Reshetov, A., Soupikov, A., and Hurley, J. (2005). Multi-level ray tracing algorithm. *ACM Transactions on Graphics (TOG)*.

Ritschel, T., Dachsbacher, C., Grosch, T., and Kautz, J. (2012). The state of the art in interactive global illumination. In *Computer Graphics Forum*.

Stich, M., Friedrich, H., and Dietrich, A. (2009). Spatial splits in bounding volume hierarchies. In *Proc. High Performance Graphics*.

Vinkler, M., Bittner, J., and Havran, V. (2017). Extended morton codes for high performance bounding volume hierarchy construction. In *High Performance Graphics*.

Vinkler, M., Havran, V., and Bittner, J. (2016). Performance comparison of bounding volume hierarchies and kd-trees for gpu ray tracing. In *Computer Graphics Forum*.

Wald, I. (2007). On fast construction of sah-based bounding volume hierarchies. In *2007 IEEE Symposium on Interactive Ray Tracing*.

Wald, I. (2012). Fast construction of sah bvhs on the intel many integrated core (mic) architecture. *IEEE Transactions on Visualization and Computer Graphics*.

Wald, I., Benthin, C., and Slusallek, P. (2003). Distributed interactive ray tracing of dynamic scenes. In *Proc. IEEE Symposium on Parallel and Large-Data Visualization and Graphics*.

Wald, I., Woop, S., Benthin, C., Johnson, G. S., and Ernst, M. (2014). Embree: a kernel framework for efficient cpu ray tracing. *ACM Transactions on Graphics (TOG)*.

Wodniok, D. and Goesele, M. (2017). Construction of bounding volume hierarchies with sah cost approximation on temporary subtrees. *Computers & Graphics*.

Yu, I., Cox, A., Kim, M. H., Ritschel, T., Grosch, T., Dachsbacher, C., and Kautz, J. (2009). Perceptual influence of approximate visibility in indirect illumination. *ACM Transactions on Applied Perception (TAP)*.

Zlatuška, M. and Havran, V. (2010). Ray tracing on a gpu with cuda–comparative study of three algorithms. *WSCG*.